JOURNAL OF MATERIALS SCIENCE **34** (1999) 4225–4231

Chemically deposited zinc oxide thin film gas sensor

A. P. CHATTERJEE, P. MITRA, A. K. MUKHOPADHYAY
Central Glass & Ceramic Research Institute, Calcutta 700032, India
E-mail: anoop@cscgcri.ren.nic.in

Zinc oxide (ZnO) thin films were prepared by a low cost chemical deposition technique using sodium zincate bath. Structural characterizations by X-ray diffraction technique (XRD) and scanning electron microscopy (SEM) indicate the formation of ZnO films, containing 0.05–0.50 μm size crystallites, with preferred *c*-axis orientation. The electrical conductance of the ZnO films became stable and reproducible in the 300–450 K temperature range after repeated thermal cyclings in air. Palladium sensitised ZnO films were exposed to toxic and combustible gases e.g., hydrogen (H_2), liquid petroleum gas (LPG), methane (CH_4) and hydrogen sulphide (H_2S) at a minimum operating temperature of 150 °C; which was well below the normal operating temperature range of 200–400 °C, typically reported in literature for ceramic gas sensors. The response of the ZnO thin film sensors at 150 °C, was found to be significant, even for parts per million level concentrations of CH_4 (50 ppm) and H_2S (15 ppm).

1. Introduction

The importance of zinc oxide (ZnO) for gas sensing applications was demonstrated in 1962 for inflammable gases [1]. ZnO gas sensors have been fabricated in various forms, such as, single crystals [2], sintered pellets [3], thick films [4], thin films [5] and heterojunctions [6]. Thin films of ZnO are expected to exhibit high degree of gas sensitivity, because the sensing mechanism involves chemisorption followed by charge transfer at the surface leading to change in resistance of the sensor element. Different methods have been applied to obtain ZnO thin films, e.g., thermal oxidation [7], chemical deposition [8], electron beam evaporation [9], activated reactive evaporation [10], spray pyrolysis [11], low pressure metal organic chemical vapour deposition (MOCVD) [12] and rf magnetron sputtering [13].

We have earlier reported the comparison of hydrogen gas sensitivity for solid state sintered, tape cast and chemically deposited thin film ZnO sensors [14]. This work established the superiority of ZnO thin film sensors over the other two competing processes of fabrication. We have recently reported also a new chemical deposition method to prepare tin-dioxide thin film gas sensors [15]. Here we report the detailed characterisation of the chemical deposition process for ZnO thin film sensors. In addition, the structural, electrical and gas sensing properties of the ZnO thin film sensors for toxic and combustible gases (H_2, LPG, CH_4 and H_2S) have been studied. The chemical deposition technique has been adopted because, it is a low cost process and the deposited ZnO films were found to be of comparable quality to those obtained by more sophisticated and expensive deposition process e.g., MOCVD. The resistance of the ZnO films in ambient air (zero level for gas sensing) was found to be stable and reproducible after couple of thermal cyclings. Surface sensitisation with palladium (Pd) ensured enhanced sensitivity; so that the ZnO thin films gave significant response to target gases at the operating temperature of as low as 150 °C, compared to the normal operating temperature range of 200–400 °C for zinc oxide resistive gas sensors [2–5].

2. Experimental

The zinc oxide thin films were deposited on glass substrates (microscope slides) by alternate dipping into sodium zincate (Na_2ZnO_2) bath kept at room temperature and hot water maintained near boiling point [8]. The glass substrates were cleaned, before deposition, by chromic acid followed by distilled water rinse and ultrasonic cleaning with equivolume mixture of acetone and ethanol. The deposited ZnO films were subsequently annealed in air at 150 °C for 15 min.

The film thickness was determined gravimetrically by measuring the change in weight of the substrate due to film deposition, the area of deposition and using the known density of ZnO (5.6 gm/cm^3). The gravimetric method has some limitations because of the non-uniformity, porosity and edge tappering effects in the chemically deposited films with a porous microstructure. However, it can give quickly the comparative data. This is the reason this method was adopted. Efforts made to take cross sectional scanning electron micrographs of the film, were not satisfactory. The deposition rate process was studied by monitoring the variation of film thickness with the concentration of Na_2ZnO_2 bath (0.03–0.125 M) and the number of immersions (25–200) in the two baths. X-ray diffraction (XRD) with

CuK_α radiation was used for studying the *c*-axis orientation and phase identification of the deposited ZnO film. Scanning electron micrography (SEM) was used to illustrate the formation of crystallites on the film surface. Prior to insertion in the sample chamber of the scanning electron microscope, the ZnO thin film was coated with a thin (∼100 Å) layer of gold to avoid charging effects.

Conductance (σ) vs. temperature (T) data were obtained in air for the temperature range 300–550 K. Approximately 30 mm long silver (Ag) contacts, separated by 5 mm, were made on ZnO films having dimensions of $3 \times 2.5\,cm^2$. The ZnO samples were heated in a tubular furnace of 3.2 cm diameter and 33 cm length. The furnace temperature was controlled within $\pm 1\,^\circ C$ and the temperature variation over the length of the ZnO films was found to be within $\sim \pm 1\,^\circ C$.

The sensitivity of the ZnO thin film sensor was studied for hydrogen (H_2), liquid petroleum gas (LPG), methane (CH_4) and hydrogen sulphide (H_2S). Hydrogen and LPG were dialuted with nitrogen (N_2) to a concentration of 2 vol% each by measuring the flow rates; while commercially available calibrated mixtures of 50 ppm CH_4 and 15 ppm H_2S in N_2 were used. To enhance the gas sensitivity, the ZnO thin films were treated with palladium by a wet chemical process [14–17]. Prior to gas exposure, the sensor was allowed to equilibrate inside the tube furnace at the operating temperature of 150 °C for 30 min. Subsequently, the target gas diluted with N_2 was allowed to flow through the tube and the sensitivity was monitored through decrease in the sensor resistance for an exposure time of 30 min. Finally, the gas flow was turned off and the sensor resistance was allowed to recover towards the initial value in air. The recovery characteristics of the ZnO thin film sensor was also monitored as a function of time.

3. Results and discussions

3.1. Film deposition

Sodium zincate bath, used for deposition of ZnO was prepared by adding sodium hydroxide (NaOH) into aqueous solution of zinc sulphate ($ZnSO_4 \cdot 7H_2O$). At first, a white precipitate of zinc hydroxide ($Zn(OH)_2$) was formed, which dissolved on further addition of NaOH thus forming the Na_2ZnO_2 bath. The reaction leading to the formation of sodium zincate is as follows:

$$Zn(SO_4) + 2NaOH = Zn(OH)_2 + Na_2SO_4 \quad (1)$$

$$Zn(OH)_2 + 2NaOH = Na_2ZnO_2 + 2H_2O \quad (2)$$

$$ZnSO_4 + 4NaOH = Na_2ZnO_2 + Na_2SO_4 + 2H_2O \quad (3)$$

The substrate is first immersed in sodium zincate bath and then the substrate with a thin layer of sodium zincate is dipped in hot water bath. This leads to the reaction

$$Na_2ZnO_2 + H_2O = ZnO + NaOH \quad (4)$$

forming a thin, porous ZnO film on the substrate. At first isolated nuclei of ZnO was formed followed by localised build-up, collapse and film growth. The film thickness was built up by increasing the number of dippings.

Details of the chemical deposition process of ZnO films were not reported earlier by Ristov *et al.* [8]. Fig. 1 shows power law dependence of film thickness (d) on the number of dippings (N) according to the following empirical equation:

$$d = KN^m \quad (5)$$

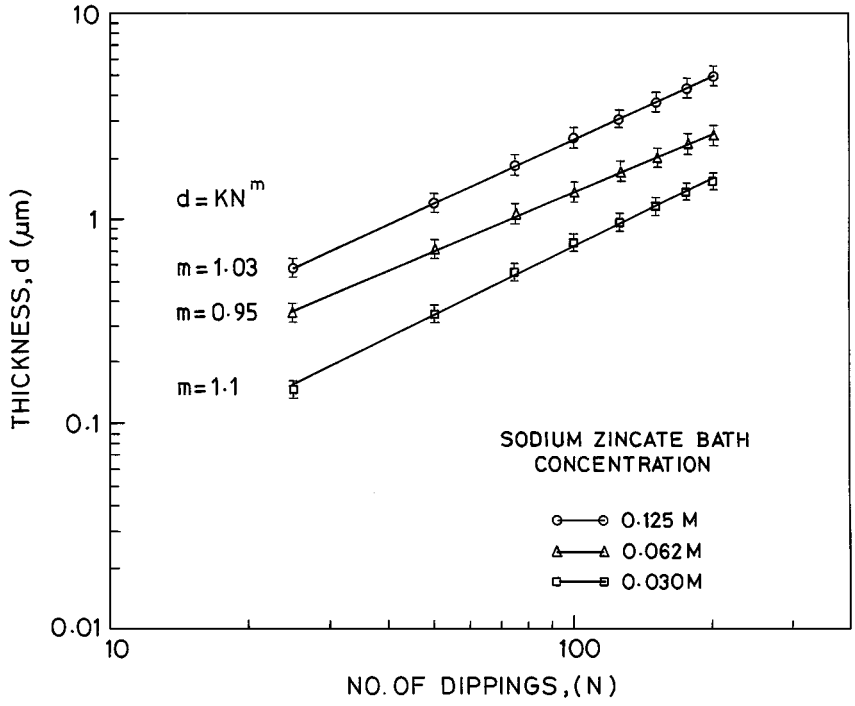

Figure 1 Chemical deposition process of ZnO thin films on glass. Film thickness d (μm) vs. number of dippings (N) in hot water (98–100 °C) and Na_2ZnO_2 bath is shown for three different concentrations (0.03, 0.062, 0.125M) of the Na_2ZnO_2 bath.

where d is the film thickness, N is the number of dippings in the two baths, m is the power law exponent and K is the growth rate constant, which varies with the concentration of the sodium zincate bath. There is a dispersion of $\pm 5\%$ in the film thickness data (shown as error bars against each data point) which probably reflects a small variability in the deposition process arising possibly from small experimental scatter in the Na_2ZnO_2 bath concentration values. Since the fit of the experimental data to Equation 1 shows $m \approx 1$ (Fig. 1), Equation 1 can be approximated as $d = KN$, where the constant K now assumes the physical significance of growth rate in (μm/dip). This implies a linear increase of ZnO film thickness (d) with increasing number of dippings (N); for three different concentrations of sodium zincate bath. Each pair of immersions in the sodium zincate bath and hot water (98–100 °C) is considered as one complete step of dip coating. The calculated values of the growth rate (K) from the data of Fig. 1 are 0.007, 0.013 and 0.025 μm per dipping for sodium zincate bath concentrations of 0.03, 0.062, and 0.125 M, respectively. Therefore, the ZnO film growth rate also scales linearly with bath concentrations. The linear nature of the chemical deposition process ensures easy control and reproducibility of predetermined film thickness. For films of thickness greater than 7 μm and for sodium zincate baths of 0.25 M concentration or greater, the growth rate became erratic and the ZnO deposition was non-uniform.

3.2. Structural characterization

Fig. 2 shows typical XRD spectra of an as-deposited and air annealed ZnO film of 2.5 μm thickness (0.125 M sodium zincate bath; 100 dippings). XRD results indicate the presence of ZnO and $Zn(OH)_2$ components in as-deposited films. The zinc hydroxide was formed due to hydrolysis of the deposited ZnO film during subsequent immersions in hot water [18]. Ristov *et al.* [8] did not report the formation of $Zn(OH)_2$ in films upto a maximum thickness of 0.85 μm. This is consistent with our observation that $Zn(OH)_2$ component could be detected by XRD for ZnO films of thickness (d) >1 μm. Single phase ZnO films were obtained by thermal annealing of the as-deposited films at 150 °C in air for 15 min (Fig. 2). This temperature of thermal anneal was obtained by the trial and error method. XRD results in Fig. 3 shows that ZnO(002) line is the strongest, indicating preferential c-axis orientation of the zinc oxide films. The variation of the degree of c-axis orientation with film thickness is shown in Fig. 4 in terms of the intensity ratio $[I(002)/I(101)]$ of ZnO(002) and ZnO(101) XRD lines. ZnO(101) is the strongest XRD line for the standard zinc oxide powdered sample and $[I(002)/I(101)] = 0.56$, is the standard value for no preferred orientation [19].

It can be seen from Figs 3 and 4 that initially the degree of orientation increases with film thickness upto $d \cong 1.2$ μm and subsequently, the degree of c-axis orientation decreases for thicker films. The onset of the loss of c-axis orientation can be attributed to the interruption of epitaxial growth due to formation of the $Zn(OH)_2$ phase for films of thickness (d) >1 μm. The dependence of the degree of orientation on film thickness was not reported earlier by Ristov *et al.* [8]. Maximum c-axis orientation of $[I(002)/I(101)] \sim 5$ (Fig. 4), for the present 1.2 μm thick ZnO film, is comparable to the degree of orientation obtained by Kim *et al.* [12] using the more complex MOCVD process (See inset of Fig. 3). Scanning electron micrograph (SEM) of the 1.2 μm thick ZnO film is shown in Fig. 5. The SEM picture clearly illustrates the formation of 0.05–0.5 μm size ZnO crystallites.

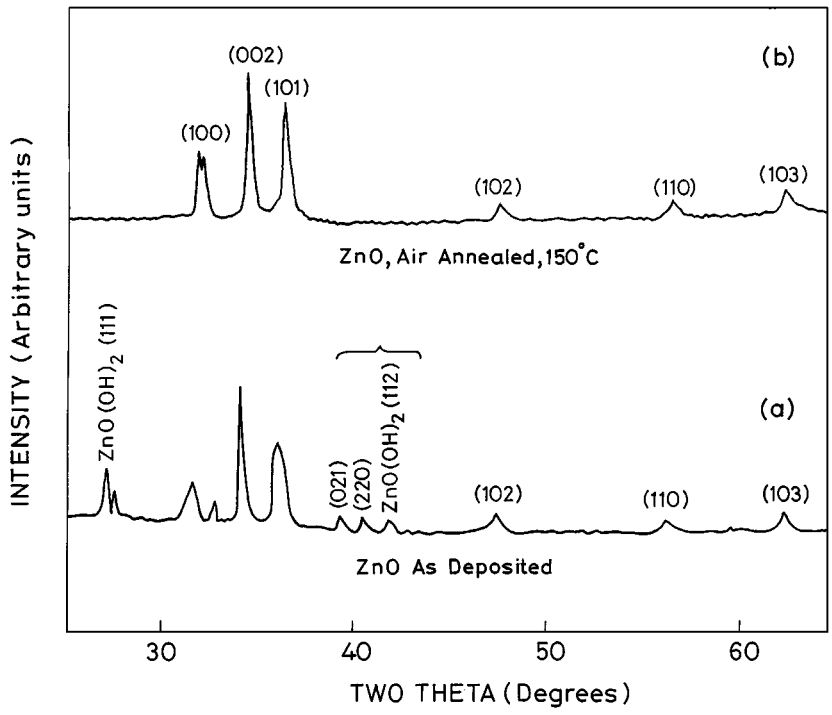

Figure 2 XRD spectra of (a) as-deposited film containing ZnO and $Zn(OH)_2$ components and (b) air annealed (150 °C, 15 min) film containing only ZnO (Film thickness $d = 2.5$ μm; $N = 100$ dippings using 0.125M Na_2ZnO_2 bath).

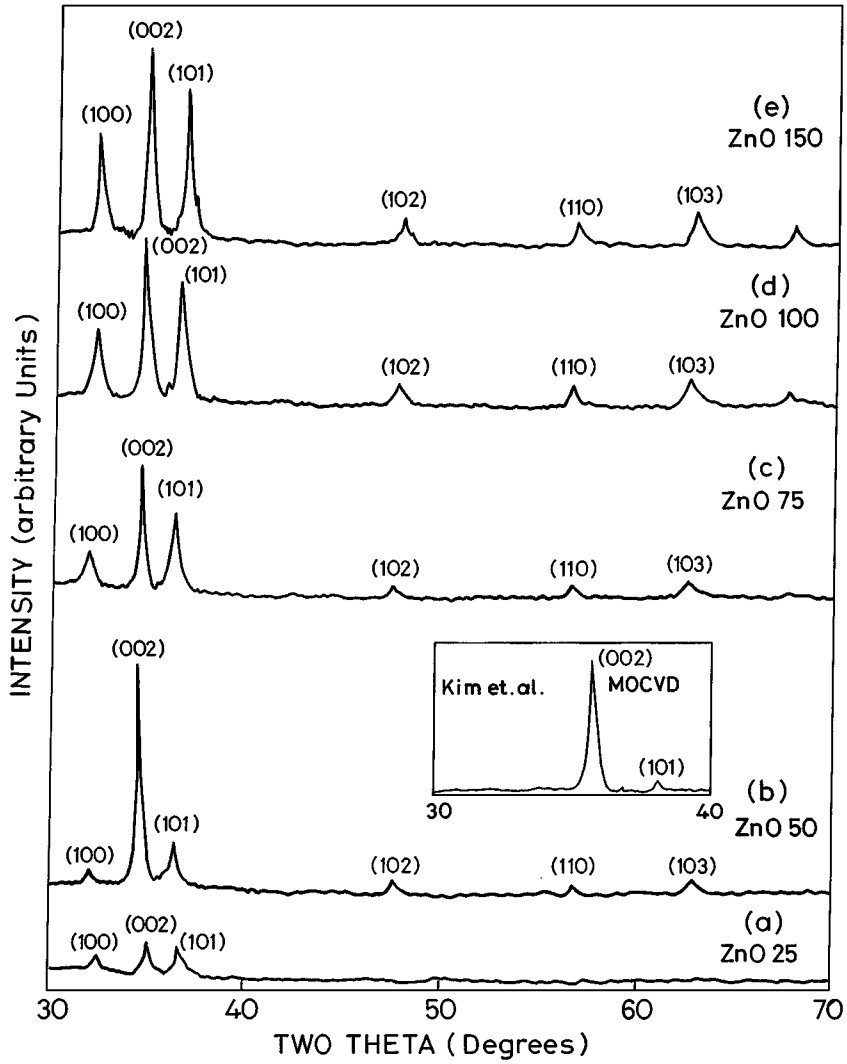

Figure 3 Series of XRD spectra showing variation in the degree of *c*-axis orientation in terms of the ZnO(002) line, for increasing film thickness with the number of dippings (a) 25, (b) 50, (c) 100 (d) 150 dippings using 0.125M Na_2ZnO_2 bath and hot water (98–100 °C). Inset shows *c*-axis orientation for ZnO films deposited by MOCVD (Kim *et al.* 1992, [12]).

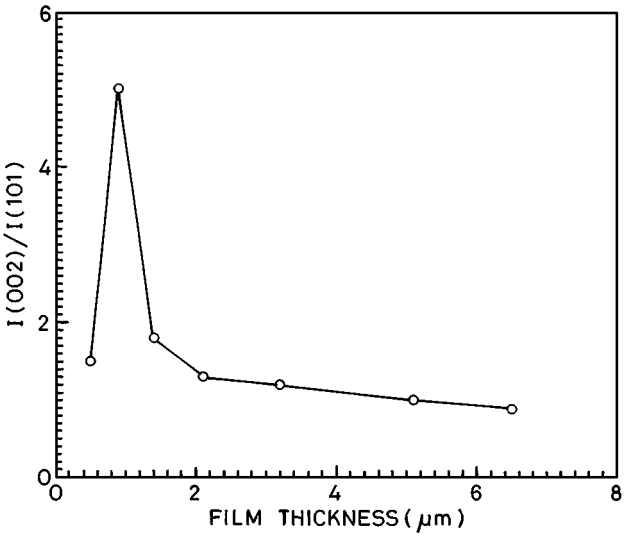

Figure 4 Variation of intensity ratio $[I(002)/I(101)]$ of ZnO(002) and ZnO(101) XRD lines with increasing film thickness. Maximum *c*-axis orientation occurred for 1.2 μm thick ZnO film.

3.3. Electrical characterisation

Temperature dependence of electrical conductance in 300–550 K range for 1.2 μm thick ZnO film, is shown in Fig. 6 for five (5) successive runs on consecutive days. The film was kept in the dark inside an enclosed tube furnace, because ZnO is known to exhibit photoconductivity [20]. Fig. 6 shows two stage conductance (σ):

$$\sigma = \sigma_{LO} \exp(-E_L/kT) + \sigma_{HO} \exp(-E_H/kT) \quad (6)$$

with activation barriers of $E_L = 0.25$–0.29 eV in the low temperature range (300–450 K) and $E_H = 1.53$–1.69 eV in the high temperature range (450–550 K). In Equation 2 σ_{LO} and σ_{HO} are the pre-exponential factors for low and high temperature conductance stages, respectively; and k is the Boltzmann constant. The low temperature activation energy is possibly associated with one of the following two donor ionisation processes:

$$V_o \rightarrow V_o^+ + e^- \quad (7)$$

or,

$$Zn_i^+ \rightarrow Zn_i^{++} + e^- \quad (8)$$

proposed by Simpson and Cordaro [21] for oxygen vacancy (V_o) and Sukker and Tuller [22] for zinc

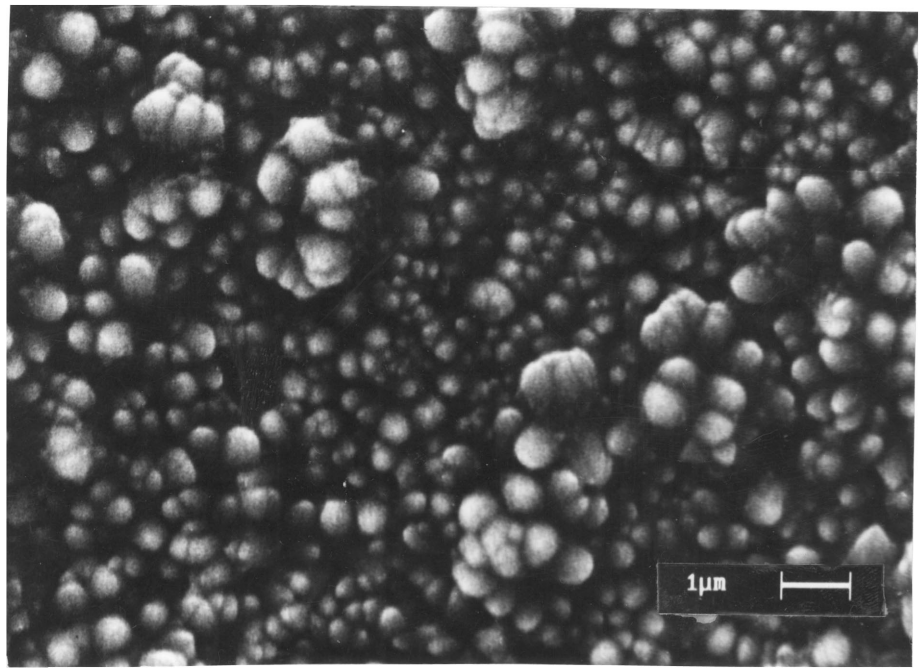

Figure 5 SEM micrograph shows 0.05–0.5 μm size crystallites in a 1.2 μm thick ZnO film having maximum *c*-axis orientation.

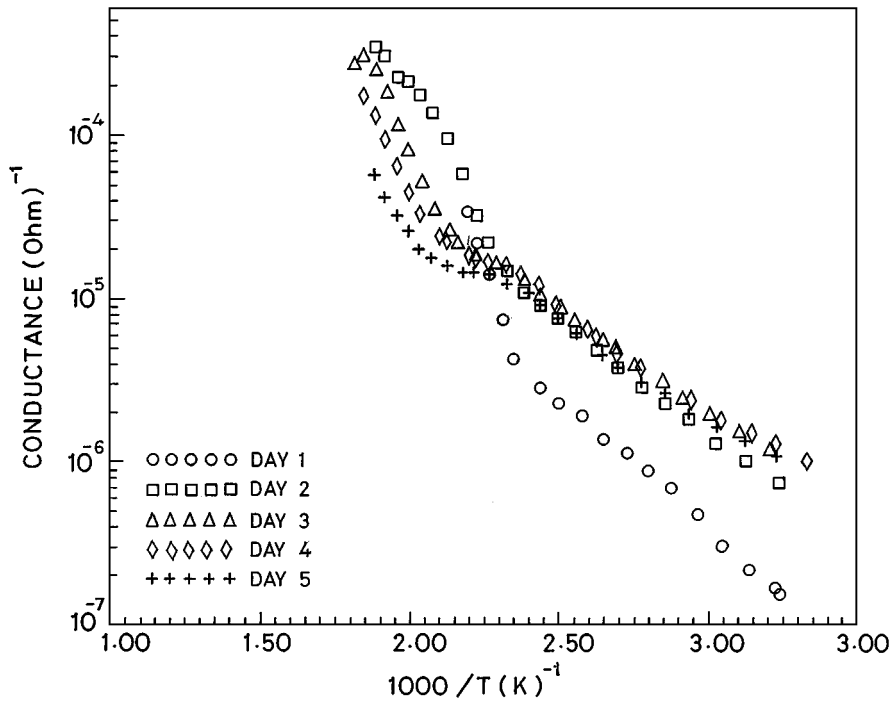

Figure 6 Temperature dependance of electrical conductance of ZnO film shows two activation barriers ($E_{LO} = 0.25$–0.29 eV in 300–450 K range and $E_{HO} = 1.53$–1.69 eV in 450–550 K range). The electrical conductance in the low temperature range stabilises during five successive runs on five consecutive days.

interstitial (Zn_i). In the low temperature range (300–450 K), the electrical conductance of ZnO thin film initially increases and then stabilised; while in the high temperature range (450–550 K), the film conductance gradually decreased during successive runs (Fig. 6). The observed conductance stabilisation in 300–450 K range is possibly due to the equilibration between oxygen chemisorption [23] and desorption [24] processes accompanied by electron transfer between adsorbed oxygen and ZnO surface:

$$O_2 + e^- \rightarrow O_2^- \qquad (9)$$

where, O_2 is gaseous oxygen and O_2^- is chemisorbed oxygen acting as an electron acceptor. The stabilisation of the ZnO film conductance in ambient air is important, because it ensures stable zero level for gas sensing applications.

3.4. Sensor characteristics

The response of the Palladium(Pd)-sensitised ZnO thin films during 30 min exposure to H_2, LPG, CH_4 and H_2S at 150 °C, is shown in Fig. 7 in terms of the reduction of sensor resistance ratio (R_g/R_a) with time. Our

TABLE I Sensing and recovery characteristics of ZnO thin film sensor

Target gas concentration (in N_2)	Time of exposure (min)	Reduced resistance ratio ($S = R_g/R_a$)	Percent reduction of resistance (S%)	Time of recovery (min)	Percent recovery of sensor
H_2 (2 vol %)	30	0.002	99.8	30	54.4
LPG (2 vol %)	30	0.069	93.1	9	100.0
CH_4 (50 ppm)	30	0.57	43.0	30	65.1
H_2S (15 ppm)	30	0.43	57.0	30	70.2

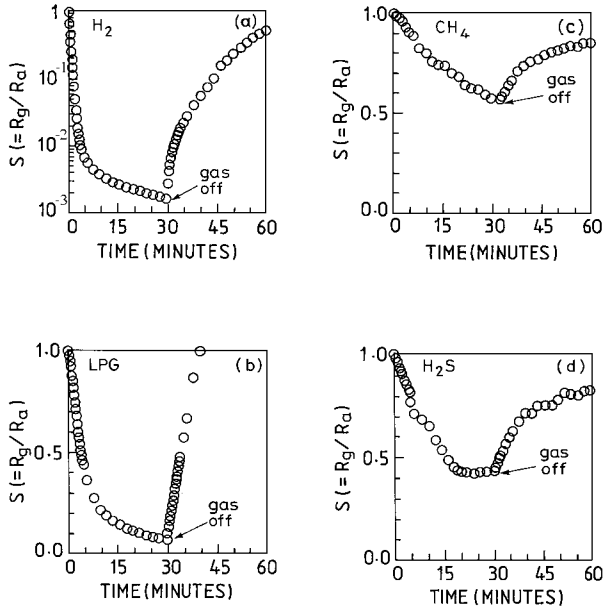

Figure 7 Sensing and recovery characteristics of ZnO thin film sensors for (a) 2 vol % H, (b) 2 vol % LPG, (c) 50 ppm CH_4 and (d) 15 ppm H_2S (all diluted with N_2). Target gas flow is turned on at $t = 0$ for gas sensing (reduction of R_g/R_a) and turned off at $t = 30$ min for recovery of the sensor (increase of R_g/R_a).

preliminary studies show [14, 17] that reasonable gas sensing action for exposure of the Pd-sensitised ZnO thin film sensor to H_2 and LPG begins at a temperature of as low as 150 °C. The sensitivity was found to increase with temperature upto 350 °C. However, to obtain comparative data for the sensor at the minimum operating temperature, so that the present ZnO thin film sensor can become less energy intensive, it was decided to do all the subsequent preliminary experiments for the four different chosen gases at 150 °C. The decrease of the ratio of ZnO thin film resistance in presence of target gases (R_g) to the corresponding film resistance in air (R_a) is a measure of the sensitivity (S):

$$S = R_g/R_a \tag{10}$$

The percent reduction of sensor resistance is also an alternative measure of gas sensitivity [25]:

$$S\% = (\Delta R/R_a) \times 100 = (1 - S) \times 100 \tag{11}$$

where $\Delta R = (R_a - R_g)$, is the decrease of sensor resistance due to exposure to target gases for a fixed time interval. The sensor has greater gas sensitivity for smaller value of resistance ratio ($S = R_g/R_a$) and larger percent reduction of resistance (S%) for a fixed exposure time to a target gas. Table I presents the data on the resistance ratios (R_g/R_a) and the S% values for 30 min exposure of the ZnO sensor to the target gases, mentioned above. The resistance of the ZnO sensor reduces by 99.8% for 30 min exposure to 2 vol % H_2 in nitrogen as compared to 93.1% decrease of the sensor resistance for exposure to identical concentration of LPG in nitrogen for the same time interval. The greater sensitivity to hydrogen is expected, because oxidation of dissociated hydrogen is faster and more effective than decomposition and oxidation of hydrocarbons (in LPG) through multistep reactions [26]. The dissociation of hydrogen takes place according to the reaction [16]:

$$H_2 + Pd^{2+} \rightarrow 2H\,(Pd^{2+}) \tag{12}$$

The oxidation of dissociated hydrogen follows from [26]:

$$4H + O_2^- = 2H_2O + e^- \tag{13}$$

However, for LPG, the reaction mechanism is quite complex and proceeds through several intermediate steps which are yet to be fully understood [25]. Significant responses to 50 ppm CH_4 ($S\% = 43$) and 15 ppm H_2S ($S\% = 57$) in nitrogen at the low operating temperature of 150 °C, clearly illustrate the high degree of sensitivity of the present ZnO thin film sensor.

The sensor resistance is expected to gradually return to its initial value in air (R_a), when the target gas flow over the sensor surface is turned off. The percent recovery (R%) of a sensor at any given time can be expressed as follows:

$$R\% = [\{\Delta R(0) - \Delta R(t)\}/\Delta R(0)] \times 100 \tag{14}$$

where $t = 0$, is the initial instant when the target gas is turned off. The recovery characteristics for the ZnO thin film sensor are also shown in Fig. 7 for exposure to H_2, LPG, CH_4 and H_2S. The sensor completely recovers ($R\% = 100$) in 9 min after 2 vol % LPG flow was turned off. The extent of recovery, observed in 30 min after the target gas flow was turned off, is also listed in Table I for the remaining three gases (2 vol % H_2, 50 ppm CH_4 and 15 ppm H_2S).

It is seen from the recovery characteristics that, the recovery is complete and fast for LPG while this is not so with the other three target gases. Although the reason behind this is not yet fully understood, it appears that in case of LPG, the reaction mechanism probably involves adsorbed oxygen species only and hence no residual species are left over to affect recovery. However, for exposure to hydrogen, the highly reactive atomic hydrogen species [4H, Equation 13] may react

with surface lattice oxygen [27]. If this be the case, then, the surface should take a reasonably long time to get back to the original resistance level as is observed in the present work. The reaction mechanism for H_2S and CH_4 is fairly complex and in this cases also the formation of atomic hydrogen is possible. However, the exact details of these complicated surface reactions are yet to be fully understood. More detailed experimentation would be necessary to substantiate the suggestions speculated here.

4. Conclusions

Controlled chemical deposition of 0.1–7 μm ZnO films, using 0.03–0.125M sodium zincate baths, is possible due to the observed linear rate of film thickness growth (d) with the number of dippings (N) as well as the sodium zincate bath concentration. The deposited ZnO films exhibit strong c-axis orientation, similar to the films prepared by more expensive MOCVD process. Stable ZnO film resistance in air (R_a) in the 300–450 K temperature range ensures reproducible zero level for gas sensing by change of resistance. Preliminary studies of gas sensing characteristics indicate that the Pd-sensitised ZnO films respond strongly to 2 vol % H_2 and LPG, which is on the lower side of the hazardous explosion ranges for H_2 (4–75%) and LPG (1.8–9%). The ZnO thin film sensors also exhibit significant response for very low concentration of CH_4 (50 ppm) and H_2S (15 ppm). The minimum operating temperature of 150 °C found in the present work is less than the previously reported operating range of 200–400 °C for ZnO resistive gas sensors. The recovery of the sensor resistance to zero level in air (R_a) is most efficient (100% recovery in 9 min) after exposure to 2 vol % LPG; so that repeated sensing and recovery cycles can be completed in quick succession. The simplicity and low cost of the present chemical deposition process, reproducibility of structural and electrical characteristics and high degree of sensitivity of the deposited film to even ppm level concentrations of toxic and combustible gases (CH_4, H_2S) make the process a front-runner for commercial production of ZnO thin film gas sensors.

Acknowledgements

The authors sincerely appreciate the keen interest of Dr. H. S. Maiti, Director, Central Glass and Ceramic Research Institute (CGCRI), Calcutta in the present work. The authors are grateful to Dr. A. K. Chakraborty and Ms. A. Laskar of CG & CRI for taking XRD spectra and SEM photograph, respectively. One of the authors (PM) is grateful to the Council of ciuentific and Industrial Research (CSIR), Government of India, for providing financial support.

References

1. T. SEIYAMA, A. KATO, K. FUJIISHI and M. NAGATANI, *Anal. Chem.* **34** (1962) 102.
2. A. JONES, T. A. JONES, B. MANN and J. G. GRIFFITH, *Sensors and Actuators* **5** (1984) 75.
3. G. UOZUMI, M. MIYAYAMA and H. YANAGIDA, *J. Mater. Sci.* **32** (1997) 2991.
4. S. PIZZINI, N. BUTTA, D. NARDUCCI and M. PALLADINO, *J. Electrochem. Soc.* **136** (1989) 1945.
5. T. YAMAZAKI, S. WADA, T. NOMA and T. SUZUKI, *Sensors and Actuators* **B13/14** (1993) 594.
6. S. BASU and A. DATTA, *ibid.* **B22** (1994) 83.
7. P. BONASEWICZ, W. HIRSCHWALD and G. NEUMANN, *Thin Solid Films* **142** (1986) 77.
8. M. RISTOV, G. J. SINADINOVSKI, I. GROZDANOV and M. MITRESKI, *ibid.* **149** (1987) 65.
9. A. KUROYANAGI, *Jpn. J. Appl. Phys.* **28** (1989) 219.
10. H. GOPALASWAMY and P. J. REDDY, *Semicond. Sci. technol.* **5** (1990) 980.
11. A. GHOSH and S. BASU, *Mater. Chem. Phys.* **27** (1991) 45.
12. J. S. KIM, H. A. MARZOUK, P. J. REUCROFT and C. E. HAMRIN, JR., *Thin Solid Films* **217** (1992) 133.
13. M. PENEZA, C. MARTUCCI, V. I. ANISIMKIN and L. VASANELLI, *Mater. Sci. Forum* **203** (1996) 137.
14. A. K. MUKHOPADHYAY, P. MITRA, D. CHATTOPADHYAY and H. S. MAITI, *J. Mater. Sci. Lett.* **15** (1996) 431.
15. A. K. MUKHOPADHYAY, P. MITRA, A. P. CHATTERJEE and H. S. MAITI, *ibid.*, in press.
16. H. YONEYAMA, W. B. LI and H. TAMURA, in "Chemical Sensors," edited by T. Seiyama (Kodansha, Tokyo, 1983) p. 113.
17. P. MITRA, A. P. CHATTERJEE and H. S. MAITI, *Mater. Lett.*, in press.
18. B. J. AYLETT, in "Comprehensive Inorganic Chemistry," Vol. 3, edited by J. C. Bailer, H. J. Emeleus, R. Nyholm and A. F. Trottman-Dickenson (Pergamon press, London, 1973) p. 187.
19. L. G. BERRY (ed.), "Powder Diffraction File" (JCPDS, Philadelphia, 1960) Card No. 5-0664.
20. S. DEVI and S. G. PRAKASH, *Pramana-J. Phys.* **39** (1992) 145.
21. J. C. SIMPSON and J. F. CORDARO, *J. Appl. Phys.* **63** (1988) 1781.
22. M. H. SUKKER and H. L. TULLER, in "Advances in Ceramics," Vol. 7, edited by M. F. Yan and A. H. Heuer (American Ceramic Society, Columbus, 1984) p. 71.
23. P. ESSER and W. GOPEL, *Surf. Sci.* **97** (1980) 309.
24. D. EGER, Y. GOLDSTEIN and A. MANY, *RCA Rev.* **36** (1975) 508.
25. H. NANTO, T. MINAMI and S. TAKATA, *J. Appl. Phys.* **60** (1986) 482.
26. G. HEILAND and D. KOEHL, in "Chemical Sensor Technology," Vol. 1, edited by T. Seiyama (Kodansha, Tokyo, 1988) p. 15.
27. S. P. S. ARYA, A. D'AMICO and E. VERONA, *Thin Solid Films* **157** (1988) 169.

Received 7 April 1998
and accepted 3 March 1999